

FLAME STRUCTURE AND SCALAR PROPERTIES IN MICROGRAVITY LAMINAR FIRES

D.A. Feikema*

NASA Glenn Research Center at Lewis Field
21000 Brookpark Road
Cleveland, OH 44135

and

J. Lim and Y. Sivathanu
En'Urga Inc.
1291-A Cumberland Avenue
West Lafayette, IN 47906

Abstract

Recent results from microgravity combustion experiments conducted in the Zero Gravity Facility (ZGF) 5.18 second drop tower are reported. Emission mid-infrared spectroscopy measurements have been completed to quantitatively determine the flame temperature, water and carbon dioxide vapor concentrations, radiative emissive power, and soot concentrations in a microgravity laminar ethylene/air flame. The ethylene/air laminar flame conditions are similar to previously reported experiments including the Flight Project, Laminar Soot Processes (LSP). Soot concentrations and gas temperatures are in reasonable agreement with similar results available in the literature. However, soot concentrations and flame structure dramatically change in long duration microgravity laminar diffusion flames as demonstrated in this paper.

Introduction

The present study of microgravity laminar diffusion flames was motivated by a requirement for improved understanding of fires in manned spacecraft. NASA's fire safety approach for manned spacecraft has been based primarily upon controlling the flammability of materials onboard and eliminating ignition sources [1-3]. To develop effective fire protection systems, the behavior of fires in various environments encountered in space exploration must be properly understood. Fire behavior and suppression processes in the space exploration missions are strongly influenced by low-gravity environments in flight and on the planetary surfaces. Thus, fire safety technology must be tailored to respond to the unusual fire characteristics in low-gravity environments [1]. The non-buoyant microgravity environment causes substantial changes in flame structure and consequently changes the properties of the produced smoke/soot. In particular, the increased residence time in the high temperature zone where the smoke/soot is formed, increases the probability that the particulate will become larger and agglomerated. Among the many technical issues to be answered, this paper addresses the issue of flame structure in a simple laminar fire including chemical composition and soot production. Thermal radiation from soot contributes to the growth and spread of unwanted fires on earth, and soot-containing plumes emitted from these flames inhibit fire-fighting efforts on earth. No less problematic are the carbon monoxide and

unburned hydrocarbon emissions that intrinsically are associated with emission from soot, i.e. carbon monoxide emissions are the main cause of fatalities in unwanted fires on earth. In quiescent microgravity (μg) environments, fires or diffusion flames are relatively weak because of the lack of buoyantly driven convective flow, and the slower resulting diffusional transport. The flame on a thick sheet or rod tends to self-extinguish under quiescent conditions [4-6]. However, there is normally a constant air circulation typically 20 cm/s inside the crew cabin which will make the μg flame stronger. The flame spread rate in μg generally increases when the oxidizer flow velocity increases.

Laminar hydrocarbon diffusion flames under microgravity conditions have shown distinct characteristics relative to normal-gravity flames. Flames are longer, up to 2 times, and larger in diameter, up to four times, and often more sooting in microgravity. This arises from the result of a significant reduction in buoyant convective forces which makes diffusion the dominant mechanism of transport. As a result, increased residence time, enhanced soot formation, radiative cooling due to larger flame size and the possible onset of a chemical kinetics limitation on heat release processes are observed [7].

Specific Objectives

The objectives of this study are to examine scalar, radiative and chemical properties of a well characterized laminar fire, i.e. the LSP flame, in short duration microgravity. The detailed results help quantify the structure of a non-buoyant laminar fire which is significant and important since fire safety technology

* Corresponding author: douglas.feikema@grc.nasa.gov
Proceedings of the 2006 Technical Meeting of the Central States Section of the Combustion Institute

must be tailored to respond to the unusual fire characteristics in low-gravity environments [8].

Experimental Methods and Instrumentation

The experiment consisted of a general purpose drop rig which was configured with a gas feed system and an ethylene laminar jet flame burning inside a chamber similar to the LSP flame [9]. The experiment package was dropped in the Zero Gravity Facility (ZGF) 5.18 second drop tower. The ethylene/air flame conditions are presented in Table 1 for a jet exit diameter of 1.65 mm. Three test cases are discussed and presented in this paper for nearly identical flame conditions. A scanning Mid-IR spectrometer, Spectraline Model No. ES100 [10, 11] was used to obtain spectrally resolved radiation measurements which enabled quantitative determination of gas temperature, CO₂ and H₂O concentrations, and soot volume fraction. Other instrumentation included a radiometer (i.e. thermopile detector), R-type thermocouple rake, top and side views from the video camera sampling at 30 Hz, and flow and pressure transducers. The flames are ignited in microgravity with a retractable hot-wire igniter approximately 0.1 seconds after the package is released. By igniting in microgravity buoyant flow is eliminated enabling the flame to evolve in a quiescent environment.

Table 1: Summary of Test Conditions for Microgravity Ethylene/Air Laminar Flame

| TEST NUMBER IN ZGF | X-12-16 | X-12-17 | X2-7-5 |
|--|----------------------|--------------------|------------|
| FUEL TYPE | Ethylene | Ethylene | Ethylene |
| NOMINAL TEST PRESSURE (kPa) | 100 | 100 | 100 |
| NOMINAL TEST TEMPERATURE (°K) | 300 | 300 | 300 |
| AVERAGE BURNER EXIT VELOCITY (mm/s) | 935 | 935 | 935 |
| INITIAL CHAMBER OXYGEN CONCENTRATION (% by Vol.) | 21 | 21 | 20.6 |
| LUMINOUS FLAME LENGTH (mm) | 56 | 55 | 51 |
| MAXIMUM LUMINOUS FLAME WIDTH (mm) | 25 | 25 | 25 |
| FUEL FLOW RATE (mg/sec) | 2.3 | 2.3 | 2.3 |
| TEST DURATION (seconds) | 5.08 | 5.08 | 5.08 |
| CHARACTERISTIC FLAME RESIDENCE TIME [9] (msec) | 120 | 120 | 120 |
| FUEL EXIT REYNOLDS NUMBER | 170 | 170 | 170 |
| PURPOSE OF TEST | Spec. Scan @ 22.5 mm | Spec. Scan @ 29 mm | TC @ 20 mm |

Figure 1 and 2 show a color side view and black/white top view of the flame after 5 seconds into the drop. The flame is quite luminous and forms a “blue”

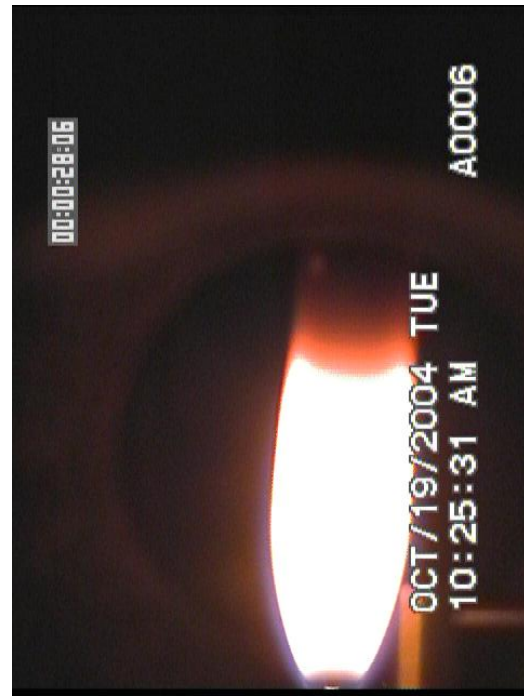


Figure 1 Side View Color Video Camera Still after 5.0 seconds for drop number X-12-17, Ethylene/Air Flame.



Figure 2 Top view Black\White Video Still after 5.0 seconds for same flame in Figure 1 showing open tip.

layer outside the glowing “yellow” soot continuum radiation region. The flame has an open tip end as seen in figure 2 and is nearly symmetric.

The flame length measurements shown in figure 3 have been taken from the side view color video camera.

Initially the flame is short at ignition and grows to attain a flame length of 55 mm on centerline after 5.0 seconds very similar to results obtained on the KC-135 parabolic aircraft. In normal gravity under buoyant conditions the same flame is 38 mm in length [9]. Under longer duration microgravity conditions, i.e. 170 seconds, the same flame increases in length to approximately 70 mm in length and reduces in width from 25 mm to 14 mm [9]. Even after 5.0 seconds the flame is still not at steady state.

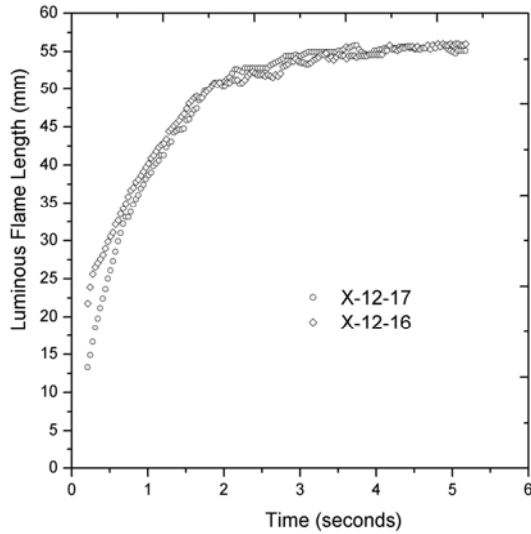


Figure 3. Luminous flame length time evolution for drop numbers X-12-16 and X-12-17, ethylene/air flame.

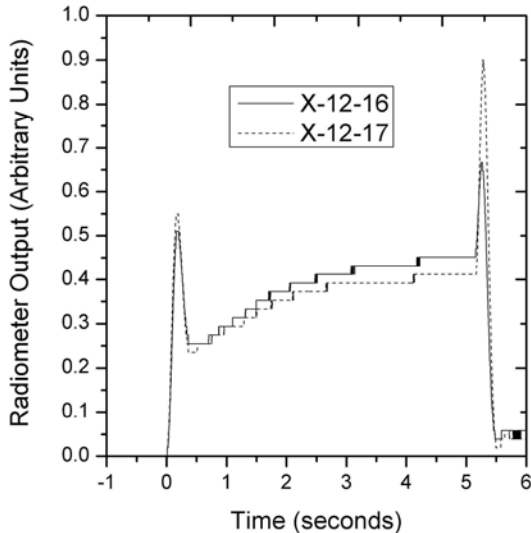


Figure 4. Radiometer Output proportional to total flame broadband spectral and continuum radiation emitted.

A spectrally broadband radiometer (ultraviolet to Infrared) was positioned inside the chamber approximately 20 cm above the nozzle and to the side of

the flame. The radiometer signal is proportional to the total flame radiation and is recorded during the drop. The results are shown in figure 4 for drops X-12-16 and X-12-17. The initial peak is the result of ignition and excess fuel gas being burnt off; however after 0.35 seconds this transient is complete and the flame begins a steady increase in flame length and in radiative output. After 5 seconds the flame radiative output has not achieved a steady state and upon impact the flame rapidly increases its radiative output before extinction.

Results and Discussion

A scanning Mid-IR spectrometer [10, 11] was positioned on the drop rig to measure radial profiles of path-integrated intensities at 160 wavelengths from 1.3 – 4.8 μm horizontally through the flame in figure 1 at two heights above the burner exit, at 22.5 mm and 29 mm. The spectrometer was outside of the chamber and the flame was viewed through a sapphire window. The spectrometer is calibrated against a black body radiation source, thus quantitative intensity measurements can be obtained. The measured intensities are shown as a contour plot in figure 5 as a function of wavelength and radial position. Radiation in the 1.3 to 3.3 μm band has contributions from both H_2O and CO_2 . Radiation in the 4.3 to 4.9 μm band has contributions only from CO_2 . Continuum radiation is also present from the radiating soot and is most evident in the 1.3 to 3.3 μm band.

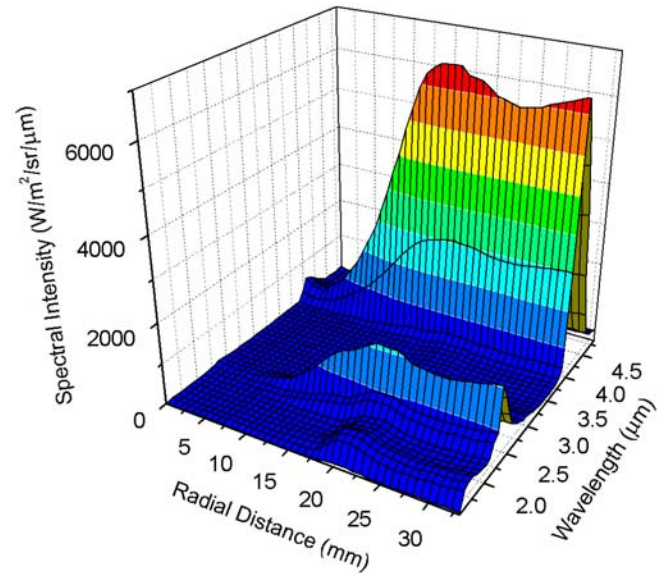


Figure 5 Contour plot of the measured intensities for drop X-12-16 in ethylene/air flame at 22.5 mm.

A deconvolution algorithm has been developed using an iterative approach to transform the measured path integrated intensities into radial profiles of gas temperature, soot concentration and both H_2O and CO_2 concentration profiles [11]. The domain is divided into

128 concentric gas layers and the flame is assumed to be symmetric which as seen in figures 1 and 2 is a reasonable assumption. The path integrated intensities have been averaged over 2.2 seconds from 2.8 to 5 seconds. After approximately 8 iterations the gas temperature is obtained and is shown in figure 6 at $x = 22.5$ mm for drop number X-12-16. The peak temperature is approximately 1725 °K at a radial position of 12.5 mm and is in good agreement with the results from the LSP experiment [9]. They report a peak temperature of approximately 1850 °K at $x = 20$ mm and 1725 °K at $x = 30$ mm. The luminous flame boundary at $x = 22.5$ mm is taken from the color video to lie at approximately 12.5 mm. For comparison reasons a normal gravity laminar ethylene/air coflow

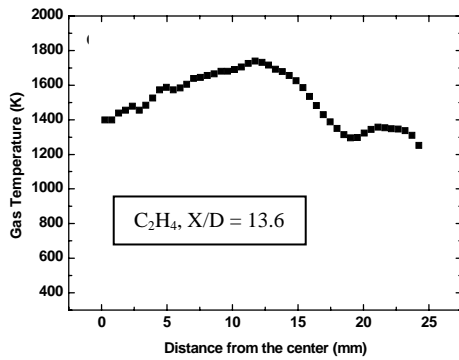


Figure 6. Temperature profile obtained in an ethylene flame at $X = 22.5$ mm (X-12-16).

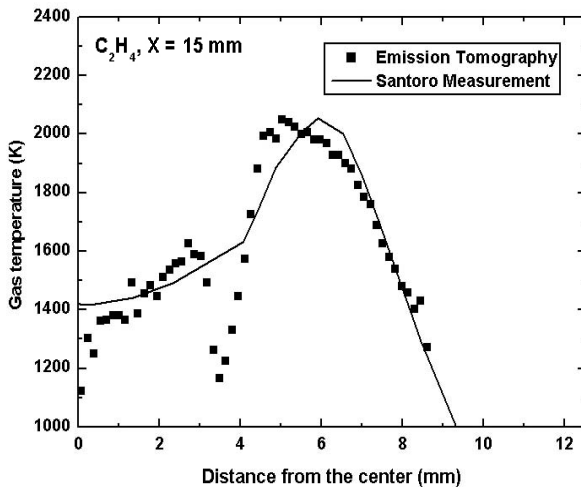


Figure 7. Thermocouple and Emission Tomography Temperature measurements in a sooting normal gravity laminar coflowing ethylene/air flame [13], fuel flow rate $3.85 \text{ cm}^3/\text{sec}$, air flow rate $713.3 \text{ cm}^3/\text{sec}$.

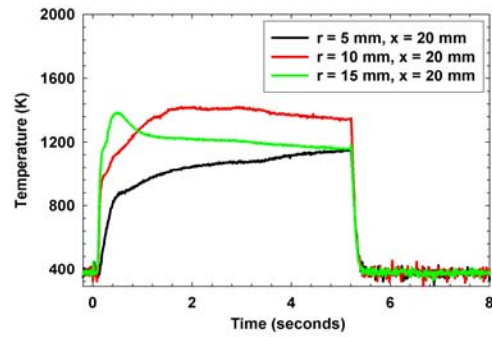


Figure 8. R-type Thermocouple Measurements (uncorrected) in ethylene flame at $X = 20$ mm and three radial locations: $r = 5, 10$ and 15 mm (X2-7-5).

flame was measured with Fan Beam Emission Tomography (FBET) and thermocouples and is shown in figure 7. The peak flame temperature is about 2050 °K at $x = 15$ mm and the reaction zone is much narrower than in figure 6.

A three channel thermocouple (TC) rake, type R platinum/rhodium alloy's, with a wire diameter of 0.003 inches and a bead diameter of approximately 0.006 inches was implemented. The thermocouple rake was positioned at a height of 20 mm above the burner and at radial locations of $r = 5, 10$ and 15 mm. Figure 8 shows the uncorrected temperature readings. The flame is disturbed somewhat by the invasive probes and is 51 mm in length rather than 55 to 56 mm without the probes. The results show that the flame does broaden as microgravity duration increases and the readings at $r = 5$ and 15 mm are nearly equal after 5 seconds in agreement with figure 6. In addition the thermocouple reading at $r = 10$ mm is higher than at 5 or 15 mm indicating that peak temperature lies between 5 and 15 mm.

Figure 9 and 10 show radial profiles of both H_2O and CO_2 mole fraction at $x = 22.5$ and 29 mm respectively.

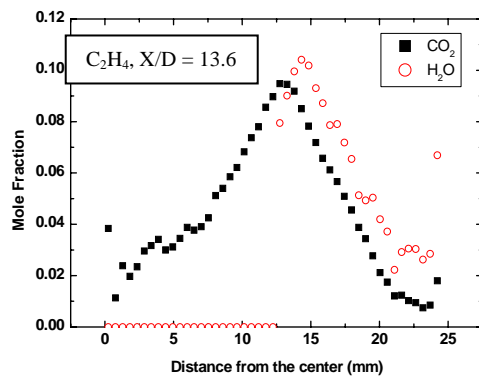


Figure 9. Gas concentration profiles obtained in an ethylene flame at $X = 22.5$ mm (X-12-16).

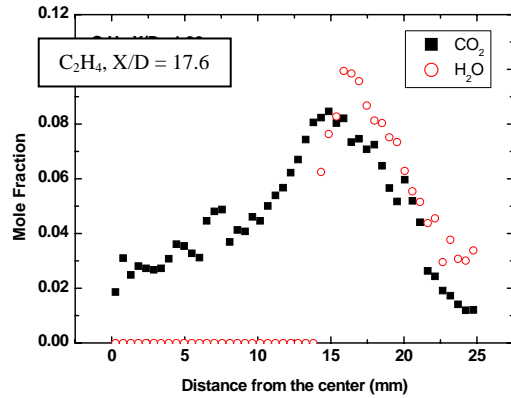


Figure 10. Gas concentration profiles obtained in an ethylene flame at $X = 29$ mm, (X-12-17).

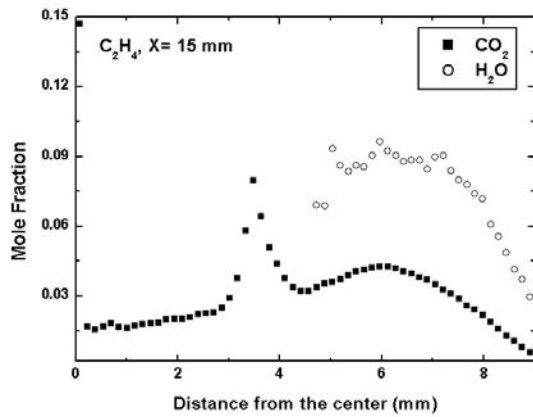


Figure 11. H_2O and CO_2 concentrations at $x = 15$ mm in normal gravity coflow ethylene/air flame, fuel flow rate $3.85 \text{ cm}^3/\text{sec}$, air flow rate $713.3 \text{ cm}^3/\text{sec}$.

The peak value of mole fraction for H_2O is approximately 0.10 and for CO_2 the peak value is approximately 0.09. Both H_2O and CO_2 concentrations at $x = 15$ mm were measured in the same normal gravity ethylene/air flame as described in figure 7 and the result is shown in figure 11. The peak value of mole fraction for H_2O is approximately 0.10 and for CO_2 the peak value is approximately 0.09 very similar to the microgravity flames. It is also observed that the flame reaction zone is narrower in normal gravity than in nonbuoyant conditions. Generalized state relationship predictions of major gas species concentrations [12] in an ethylene/air diffusion flame are shown in table 2. The measurements are within 20% of this value.

Table 2 Summary of State Relationship [12] Mole Fractions for Ethylene/Air Flame initially at Standard Temperature and Pressure

| ϕ | X_{N_2} | X_{O_2} | X_{CO_2} | X_{CO} | X_{H_2O} | X_{H_2} |
|--------|-----------|-----------|------------|----------|------------|-----------|
| 1.0 | 0.7187 | 0.0212 | 0.1033 | 0.0244 | 0.1227 | 0.0098 |

The radial profiles of soot volume fraction have been determined from the continuum radiation present in the path integrated intensities and are shown in figures 12 and 13 at $x = 22.5$ and 29 mm respectively.

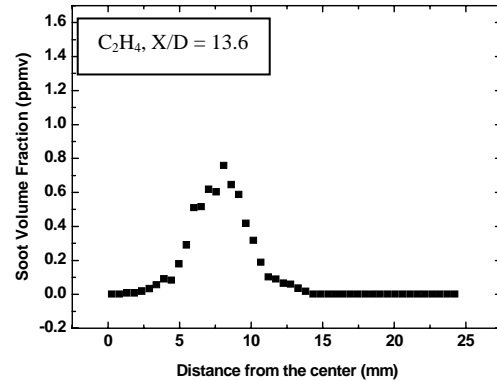


Figure 12. Soot volume fraction profile obtained in an ethylene flame at $X = 22.5$ mm (X-12-16).

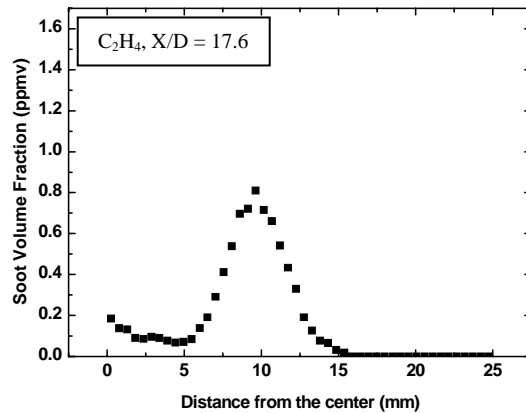


Figure 13. Soot volume fraction profile obtained in an ethylene flame at $X = 29$ mm (X-12-17).

The peak value is about 0.8 ppm at 8 to 10 mm radial position. The soot peak lies on the fuel rich side of the flame and in the preheat region. This is much lower than measurements reported previously in microgravity flames. For validation and comparison reasons the soot volume fraction was measured in a normal gravity sooting ethylene/air flame in a Santoro type coflow laminar burner with fuel flow rate of $3.85 \text{ cm}^3/\text{sec}$. As shown in figure 14, at $x = 15$ mm the peak soot volume fraction was measured to be 3 ppm at a 4 mm radius. The soot layer is much narrower, i.e. 2 mm, as compared with the 5 second drop test which is 5 mm thick. Also, soot measurements were made in a long duration microgravity ethylene/air flame or LSP experiment [9]. The peak soot concentrations in the LSP experiment were approximately 5 ppm at $x = 20$ mm and 8 to 12 ppm at $x = 30$ mm with microgravity duration times of 90 and 170 seconds. The width of the soot layer in the LSP experiment was about 2 mm at $x = 20$ and 30 mm.

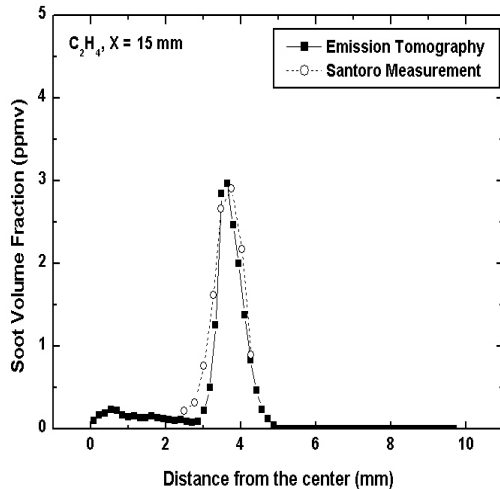


Figure 14. Laser extinction [14] and Emission Tomography Soot Volume measurements in a normal gravity sooting laminar ethylene/air flame at 15 mm above burner, fuel flow rate $3.85 \text{ cm}^3/\text{sec}$.

Conclusions

The following conclusions can be obtained from the study.

1. A Fan Beam Emission Tomography (FBET) system to obtain spectral radiation intensities at several wavelengths and at several view angles from laminar flames was successfully implemented in microgravity.
2. The laminar microgravity ethylene/air jet flame has a broader reaction zone, has a longer luminous flame length, and is cooler than a similar normal gravity flame. This is in agreement with Bahadori et al. [7].
3. The soot layer in microgravity after 5 seconds duration is 5 mm which is thicker than in normal gravity, i.e. 2 mm. For longer microgravity duration, i.e. 170 seconds, the flame shape changes to be longer and narrower and the soot layer reduces to about 2 mm thickness.
4. The peak mole fractions for H_2O and for CO_2 estimated using FBET are in agreement with the values derived from generalized state relationships for ethylene/air diffusion flames.

Acknowledgements

This work is supported by NASA under contract No. NAS3-01085.

References

1. Freidman, R., "Fire Safety in Extraterrestrial Environments", NASA/TM-1998-207417, 1998.
2. Freidman, R., Fire Safety in the Low-Gravity Spacecraft Environment, NASA/TM-1999-209285, 1999.

3. Freidman, R. and Ross, H. D., "Combustion Technology and Fire Safety for Human-crew Space Missions", In *Microgravity Combustion: Fire in Free Fall*, (H.D. Ross Ed.) Academic Press, San Diego, 2001, p.525-562.
4. Olson, S. L., "Fuel Thickness Effects on Flame Spread and Extinction Limits in Low Gravity as Compared to Normal Gravity", Eastern Section/The Combustion Institute Meeting, 1991.
5. Egorov, S. D., Belayev A., Yu., Klimin, L. P., Voiteshonok, V. S., Ivanov, A. V., Semenov, A. V., Zaitsev, E. N., Balashov, E. V., Andeeva, T. V., "Fire Safety Experiments on "Mir" Orbital Station", Third International Microgravity Combustion Workshop, NASA CP-10174, 1995, pp. 195-199.
6. Ivanov, A. V., Balashov, Ye. V., Andreeva, T. V., Meilikhov, A. S., "Experimental Flammability in Space", NASA CP-199-2094505, 1999.
7. Bahadori, M. Y., Stocker, D. S., Vaughan, D. F., Zhou, L., and Edelman, R. B., "Effects of Buoyancy on Laminar, Transitional, and Turbulent Gas Jet Diffusion Flames", Chapter 4 in *Modern Developments in Energy, Combustion and Spectroscopy*, Editors: Williams, F.A., Oppenheim, A. K., Olfe, D.B., and Lapp, M., Pergamon Press, pp. 49-66, 1993.
8. Ruff, G. A., Urban, D. L., and King, M. K., "Fire Prevention, Detection, and Suppression Research Supporting Manned Space Exploration: One Year Later", AIAA-2006-0347, Reno, Nevada, 2006.
9. Urban, D. L., Yuan, Z.-G., Sunderland, P. B., Linteris, G. T., Voss, J. E., and Faeth, G. M., "Structure and Soot Properties of Nonbuoyant Ethylene/Air Laminar Jet Diffusion Flames", AIAA Journal, Vol. 36, No: 8, pp. 1346-1360, 1998.
10. Lim, J., Sivathanu, Y., Feikema, D. A., "Fan Beam Emission Tomography", AIAA-2006-0436, Reno, Nevada, 2006.
11. Lim, J., Sivathanu, Y., and Gore, J., "Estimating Scalars from Spectral Radiation measurements in a homogeneous gas layer", Combustion and Flame, Vol. 137, pp. 222-229, 2004.
12. Sivathanu, Y. and Faeth, G. M., "Generalized State Relationships for Scalar Properties in Nonpremixed Hydrocarbon/Air Flames, Combustion and Flame", Vol. 82, pp. 211-230, 1990.
13. Santoro, R. J., Yeh, T. T., Horvath, J. J., and Semerjian, H. G., "The Transport and Growth of Soot Particles in laminar Diffusion Flames", Combustion Science and Technology", Vol. 53, pp.89-115, 1987.
14. Santoro, R. J., Semerjian, H. G., and Dobbins, R. A., "Soot Particle Measurements in Diffusion Flames", Combustion and Flame, Vol. 51, pp203-218, 1983.